A Mixed Combinatorial Optimization model for the Río Negro Hydroelectric Complex

Claudio Risso[1] [0000-0003-0580-3083], Sergio Nesmachnow[1] [000-0002-8146-4012], Rodrigo Porteiro[2] [0000-0001-7793-1645], J. Mario Vignolo[1], Emiliano Sierra[2], and Mario Ibarburu[2]

[1] Facultad de Ingeniería, Universidad de la República (UdelaR), Uruguay
{crisso,sergion,jesus}@fing.edu.uy
[2] UTE, Administración Nacional de Usinas y Trasmisiones Eléctricas, Uruguay
{rporteiro,esierra,mibarburu}@ute.com.uy

Abstract. The management of power generation systems requires the optimized coordination of resources and investments across timeframes ranging from days to decades. This paper introduces a mixed-integer optimization model (MIP) for the short-term operation of the Río Negro Hydroelectric Complex, a crucial asset in Uruguay's efforts to achieve energy sovereignty by primarily relying on wind, solar, and hydroelectric power sources. The model addresses the challenge of balancing fluctuating renewable energy supply with hydroelectric resources while ensuring cost-effective dispatch and system reliability. The experimental results demonstrate the accuracy with which a MIP approximation can model an extremely nonlinear problem.

Keywords: energy optimization, hydrothermal dispatch, mixed integer linear programming

1 INTRODUCTION

Managing the generation power system involves optimizing over different time horizons spanning from days to several decades. The complexity of this management arises from the large number of components and decisions involved, and from the uncertainty in key parameters. Technological advancements and environmental protection initiatives can influence the management of an electrical system. The issue is explored through an analysis of the Uruguayan electricity system, which has become a global reference after achieving energy sovereignty, relying heavily on renewable energy sources to meet its electricity demand [1, 3]. Uruguay has demonstrated remarkable capacity in integrating these energy sources into its electrical matrix, achieving a balance between efficiency and sustainability. This paper presents a mixed-integer optimization model (MIP) for energy production in the Río Negro Hydroelectric complex, which has been a cornerstone in the successful renewal of Uruguay's electrical system. This complex is bound to play a key role in adapting the system to future challenges, serving as a central element in the country's strategy to maintain its leadership in the use of clean energy and efficient planning of the electrical system.

1.1 Integration of non-conventional renewable energy and its impact on the energy system

Between 2017 and 2020, Uruguay successfully supplied over 95% of its energy demand through renewable generation, with minimal dependence on fossil fuels [12]. This achievement results from the country's strategic approach in balancing its existing controllable hydroelectric capacity with new investments in non-conventional renewable energy sources.

In 2021 and 2022, Uruguay continued to meet its domestic energy needs predominantly with renewables [15]; however, approximately 20% of its electricity production during this period came from thermal fossil sources. This shift was largely due to an unusual drought in Southeastern South America, which severely affected major hydroelectric plants in the region. Despite these conditions, Uruguay exported electricity to Argentina and Brazil (see Figure 1) to help meeting their energy demands, substantially increasing its production beyond internal consumption.

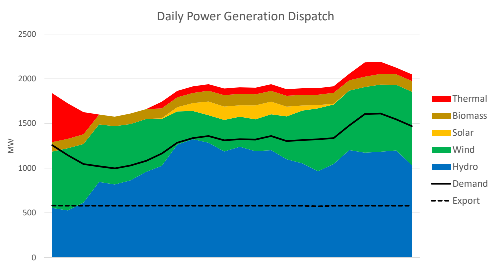

Fig. 1. Daily dispatch with an abundance of renewables and export (October 8, 2021).

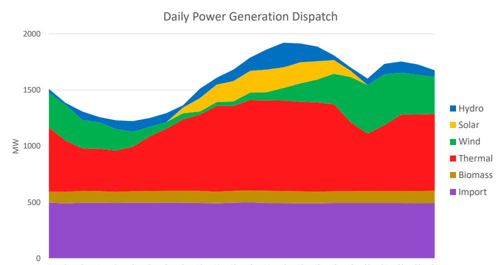

Fig. 2. Daily dispatch with renewable shortages and high imports (March 8, 2023).

In 2023, the drought severely impacted the Uruguayan hydroelectric generation, which on average accounts for over 40% of the country's energy supply. To address this shortfall, Uruguay increased its reliance on thermal generation to meet domestic demand, while also importing energy, primarily from Brazil. This notable shift in energy exchange conditions is reflected in the contrast between Figure 1 and Figure 2. The inter-annual variability in water inflows is one of the main features of the Uruguayan power system [11]. Moreover, hourly power supply from existing wind and solar power plants is highly volatile as in most power systems. In this context both the managing of water resources stored in hydro power plants reservoirs and power exchanges with neighboring systems (Argentine and Brazil) are of paramount importance for the system.

Thermal plants and power imports must fill the gap as hydro decreases, introducing two sources of inter temporal restrictions: i) the startup time of the largest and most efficient thermal units which requires up to 24 hours to achieve full power; ii) the conditions of power trade with Brazil, based upon a portfolio of short-term offers. Each offer has a term during which energy can be bought, a limited activation window before unaccepted offers expire, and once accepted a minimum amount of energy to be purchased. Offers' terms often extend longer than a week. Hence, Uruguay's short-term planning horizon has been extended to incorporate periods of up to fifteen days, to account for those restrictions. The perspective of rapid demand growth in emerging sectors such as electric vehicles [10] and hydrogen production [2] could introduce greater flexibility into energy management but also add complexity to planning models. We outline the types of problems, the case study, and the hypotheses on which this work is based.

1.2 Frameworks for Electric System Operation and Planning

Electric system management is divided into different time horizons, with problems being solved sequentially in reverse order from how they are presented here.

Continuous-Time Grid Control: It is the continuous-time grid control, where real-time production is coordinated among a predefined set of generating units to meet demand at every moment, ensuring that network frequency, active/reactive power flow, and other physical parameters remain within limits [8]. This is primarily an electrical engineering challenge and lies outside the scope of this paper.

Unit Commitment and Dispatch Optimization: It is the short-term operation planning problem. The objective here is to determine which generating units will be started up or stopped over the next few days, and how much power each plant should produce hourly to meet the demand with the least cost. This process defines the set of units that will be controlled in the continuous grid control model mentioned earlier. Dispatch planning relies on cost data, short-term forecasts or scenarios for demand, water inflows to reservoirs, hourly power from uncontrollable sources like wind and solar, cross-border energy trading with neighboring countries and scheduled maintenance of generating units [5]. Typically, the dispatch horizon spans between 48 hours and 480 hours, divided into hourly intervals, and is updated multiple times per day to adjust for the latest forecast data. This paper primarily focuses on addressing this type of short-term problem. To optimize the short-term operation problem, it is necessary an approximation of the Bellman value function at the end of the short-term horizon [7], which gives the least expected cost of longer-term operation thereafter.

Medium- and Long-Term Planning Models: This level involves medium- and long-term operation planning models. In many power systems, hydro power plants have large reservoirs which when full can store water to maintain the plant production for weeks, months or years without using the water inflows. Medium- and long-term operation planning models, which cover horizons ranging from a few weeks to several years, aim to assign value to strategic assets, such as the water stored in reservoirs [6, 14]. These values are transmitted to short-term models by means of Bellman value function approximations.

Investment Decision Models: Finally, very long-term models simulate the electric system over several decades, adding to the random variables aforementioned, others like fossil fuel prices, and technology costs. These models evaluate the economic outcomes of system operations over extended periods and are out of the scope of this work.

UTE has developed a set of systems to manage the previous problems, including MOP [9], a model for the short and medium term operation and Mingo, to optimize generation investment. This work is part of a joint venture between UTE and UdelaR, exploring the use of MIP models as an alternative approach for addressing short-term operations. The remainder of the document focuses exclusively on the unit commitment and dispatch problem, treating the grid as a single node and excluding complexities such as international energy transactions.

1.3 Case study: Simplification of Uruguay's Electric System

While the specifics of the thermal units are not addressed in detail, the hydroelectric facilities are thoroughly examined, as the primary subject of this study. Figure 3 illustrates the layout of the four dams that comprise Uruguay's hydroelectric complex. Complementarily, Table 1 shows its main parameters. For

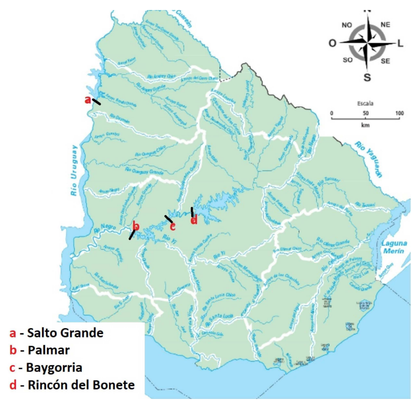

Fig. 3. Map of Uruguay with the 4 hydroelectric plants of the system

Name of the Unity	Maximum Power	Days to empty	Source of the inflows
Bonete	149MW	182	Río Negro
Baygorria	111MW	3	Bonete [+8h] and others
Palmar	343MW	13	Baygorria [+16h] and others
Salto Grande	1890MW	15	Río Uruguay

Tab. 1. Technical parameters of hydroelectric plants in Uruguay

dispatch planning purposes, the future cost function (Bellman values) is an input derived from medium and long-term planning models.

Before 2005, electricity demand was met using a combination of hydroelectric plants and controllable thermal units. As shown in Table 1, starting from its maximum water level and operating at full capacity, the Rincón del Bonete power plant has an estimated depletion period of six months, assuming no natural inflows to replenish the reservoir (i.e., no hydrological inputs). The Bonete reservoir, notable for its size, was once the largest artificial lake in the world for several years following its inauguration in 1945. Together with the two downstream hydroelectric plants on the same river: Baygorria and Palmar, it constitutes Uruguay's primary energy storage system. The ability to function as a large energy accumulator has enabled the effective integration of non-conventional renewable energy sources in Uruguay, potentially reducing the reliance on batteries to manage the intermittency of solar and wind energy. If they generate more energy than expected, hydroelectric production is scaled back, allowing reservoirs to store the surplus energy indirectly through water reserves. Conversely, when renewable generation falls short of forecasts, hydroelectricity compensates.

In 2005, Uruguay embarked on a substantial investment in non-conventional renewable energy sources, among which, biomass (mainly pulp mills) stands out due to their controllability and operation, which closely resemble traditional thermal plants but without the reliance on fossil fuels. Simultaneously and because of country's favorable conditions, Uruguay saw a considerable expansion of wind farms, reaching a combined installed capacity of 1500 MW, and more recently solar energy, whose installed capacity has reached 250 MW. The fossil fuel-based thermal generation capacity currently stands at 1154 MW. Around 36% of Uruguay's installed capacity comes from non-dispatchable sources, whose intermittence presents significant challenges for system dispatch planning.

Prior to 2005, Uruguay's electricity generation was predominantly controllable. Within a 72-hour planning horizon, both hydrological inflows and national electricity demand could be forecasted with high accuracy, and short-term planning systems were inherently deterministic. With the integration of wind, solar, and biomass, these sources are prioritized, supplying electricity as long as it does not exceed demand. Controllable components then meet the residual demand: the gap between total demand and non-conventional renewable generation.

The volatility of renewables shifts to this residual demand, becoming the key variable in dispatch models. This rapid growth of non-conventional energy sources has driven a significant redesign of short- and medium-term planning systems. Short-term planning currently uses Stochastic Dynamic Programming [4], crucial to Uruguay's energy transition. However, new challenges arise, including managing flexible demands, complex thermal unit commitments, and the increasing role of international energy exchanges. Large amounts of wind and solar capacity increase the level of uncertainty of the problem and the need of methods to take it into account [16]. One of the ways to address this problem is through the use of a Mixed-Integer Stochastic Programming (MISP) approach. A notable example of this is the case of [13], which serves as a direct reference for such implementations. MISPs are well suited to deal with a small power system like the Uruguayan one. Conversely, the non-linearities of hydroelectric plants, especially in the Río Negro basin, complicate linear optimization models, as lake states affect production. This paper presents a MIP model to optimize dispatch costs for the Río Negro hydroelectric complex, accounting for system failures: a fine for not being able to fulfill demand. For sake of simplicity, the model assumes known residual demand and hydrological contributions over the next fifteen days.

2 PRODUCTION MODEL FOR THE RÍO NEGRO

The Río Negro Hydroelectric Complex houses three of the four hydro-generation units of Uruguay. It is of utter importance the fact that these three electric dams are in tandem in the following sequence: Bonete, Baygorria and Palmar. The outflows from Bonete are integrated into the stock of Baygorria's lake after an 8-hour delay, while the outflows from Baygorria reach Palmar's lake after 16 hours. The actual production function of a hydroelectric unit is complex and depends on countless variables. A reference production function of a hydroelectric unit is

$$P = \rho g \eta \cdot Q^{trb} \cdot (h^{lk} - h^{rv}). \tag{1}$$

The formulation in Eq. (1) relies on the efficiency of turbines and the potential energy at the height of the reservoir's lake, where P corresponds to the generated power [MW], Q^{trb} to the water flowing downstream through the turbines [m^3/s], h^{lk} is the height of the top of the lake and h^{rv} is the level of the river after the dam, both expressed in [m]. $(h^{lk} - h^{rv})$ is the head of the dam. Remaining parameters are constants, namely: the Earth's gravitational acceleration g [m/s^2]; the density of water ρ [kg/m^3]; the energy conversion efficiency of turbines η [dimensionless]. In this model, the state variable h^{lk} solely depends on the volume of water at the reservoir. The height of Bonete and Palmar lakes can be adjusted with degree two polynomials at a relative error lower than 1%. Baygorria is operated as a run-of-the-river hydroelectric generator, so that water coming from upstream is either turbinated or spilled at that moment.

Regarding control variables, besides turbinated water Q^{trb}, another source of water discharges to account for is the spilling Q^{spl}. At times, either for security reasons or simply for profitability, water must be released from the dam without generating power. To fully account water discharges Q^{wds}, both components are included, since $Q^{wds} = Q^{trb} + Q^{spl}$. Water discharges raise the level downstream (i.e., h^{rv}), which, according to (1), decreases the productivity of water passing through the turbines. This level is also affected by the height of the next lake downstream, if one exists. Therefore, the river height downstream Palmar depends only on its water discharges, Baygorria's river h^{rv}_{Bay} depends on its own discharges Q^{wds}_{Bay} and on the height h^{lk}_{Pal} of Palmar's lake:

$$h^{rv}_{Bay} = F_R(h^{lk}_{Pal}, Q^{wds}_{Bay}). \tag{2}$$

Baygorria's lake is constant in height (run-of-the-river unit), so Bonete's river depends only on its discharges Q^{wds}_{Bon}. Downstream rivers height can be approximated by linear functions or degree two polynomial. Such interdependencies end up linking production variables of some units with state variables of others. The Río Negro Complex must be optimized as a whole.

2.1 Formulation and Parameters Adjustment

To adjust all these functions, UTE provided us with the complete hourly time series for the Río Negro, covering production, control, and state variables, as well as natural inflows, over a ten-year period from January 1$^{\text{st}}$, 2010, to December 31$^{\text{th}}$, 2019. The final adjustment and formulation are in the polynomial of Eq. (3), which renames control and state variables for sake of simplicity.

$$
\begin{aligned}
P(x_{1h}, y_{1h}, v_{1h}, x_{2h}, y_{2h}, x_{3h}, y_{3h}, v_{3h}) = \sum_{t=1}^{T} & p_1^{(1)} x_{1h,t} + p_1^{(2)} x_{1h,t} v_{1h,t} - p_1^{(3)} x_{1h,t} v_{1h,t}^2 \\
& - p_1^{(4)} x_{1h,t}^2 - p_1^{(4)} x_{1h,t} y_{1h,t} + p_2^{(1)} x_{2h,t} - p_2^{(2)} x_{2h,t}^2 - p_2^{(2)} x_{2h,t} y_{2h,t} - p_2^{(3)} x_{2h,t} v_{3h,t} \\
& + p_2^{(4)} x_{2h,t} v_{3h,t}^2 + p_3^{(1)} x_{3h,t} + p_3^{(2)} x_{3h,t} v_{3h,t} - p_3^{(3)} x_{3h,t} v_{3h,t}^2 - p_3^{(4)} x_{3h,t}^2 \\
& - p_3^{(4)} x_{3h,t} y_{3h,t} + p_3^{(5)} x_{3h,t}^3 + p_3^{(5)} x_{3h,t} {y_{3h,t}}^2 + 2 p_3^{(5)} {x_{3h,t}}^2 y_{3h,t},
\end{aligned} \tag{3}
$$

Subscripts $1h$, $2h$ and $3h$ allude to hydraulic units, respectively Bonete, Baygorria and Palmar. Constants $p_i^{(j)} \geq 0$ are the coefficients for the production of each unit $1 \leq i \leq 3$. Variable names x, y and v respectively refer to turbinated flow [m^3/s], spilling [m^3/s] and lake's volume [m^3] at each unit. It is assumed that variables are discretized into time-slots of equal length, of one hour in this case, along a time-horizon of T hours. While the result of the sum in Eq. (3) accounts for the whole energy [MWh] produced during the period, each addend captures the energy production at its time slot. To assess the quality of some regressions, Figure 4 presents the real-world data (in red) for the height of each lake along a reference year (2011), compared with the result of regressions (in blue).

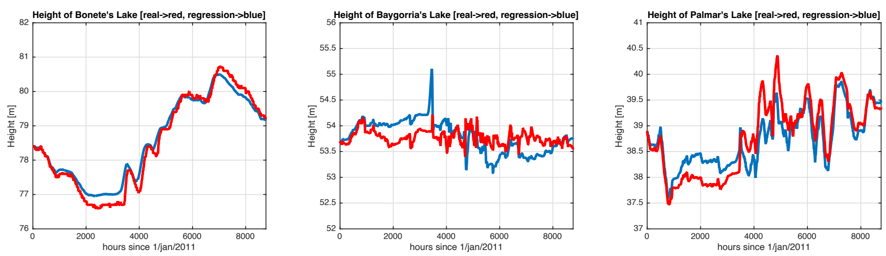

Fig. 4. Records and estimations for the height (over sea level) at each lake over the Río Negro along 2011.

Considering that some input-data (e.g., natural inflows) have sampling errors, and other variables affecting the result (e.g., wind speed and direction) were disregarded for lack of data, the overall result is quite remarkable. After computing the differences between the model in equation Eq. (3) and the actual power series during 2011, is noted that: i) 79.5% of the samples have an absolute error below 6 MW, which is 1% of the combined capacity of the Río Negro's power plant; ii) this figure increases to 92.9% when the absolute error is below 12 MW (i.e., 2% of the plant); and iii) the regression was based on data from the entire ten-year period, during which several turbines were offline during days due to scheduled maintenance or malfunctions, affecting the nominal production.

In summary, we conclude that the non-linear reference model in Eq. (3) is highly accurate overall.

2.2 Medium-term Optimization Reference

The reference production model in Eq. (3) is a differentiable function, but the Hessian matrices of these polynomials are generally not definite (i.e. neither convex nor concave) on a slot-by-slot basis, which poses a significant challenge for conventional optimization techniques. The first step in addressing the problem is to find solutions that allow optimizing energy production in a long-term reference context of one year. The goal is to get insights of an ideal operation for a specific context. The year 2011 was selected as the reference because it had the lowest water inflows to the Río Negro basin during the ten-year period. This required near-optimal use of water reserves, providing insights to simplify the general model. The non-linear problem addressed in this section is

$$\begin{cases} \max\limits_{X,Y,V} P(X,Y,V) \\ d_t \geq P_t(X_t, Y_t, V_t), \quad (i) \\ (X,Y,V) \in F. \qquad (ii) \end{cases}, \tag{4}$$

where $P(X,Y,V) = \sum_{t=1}^{T} P_t(x_{1h,t}, y_{1h,t}, v_{1h,t}, x_{2h,t}, y_{2h,t}, x_{3h,t}, y_{3h,t}, v_{3h,t})$, being $P_t(X_t, Y_t, V_t)$ the addends/terms in the sum of Eq. (3). For the system to be operational, the flows of water through the turbines (X), the spillways (Y), as well as the water volume in the reservoirs (V), must stay within technical limits, expressed in Eq. $(4)-(ii)$ in the form of a set F. Additionally, at each time step t, the power P_t generated and supplied to the grid cannot exceed the demand d_t of that period (Eq. $(4)-(i)$). The volume of water in each reservoir at any time must always comply a mass balance equation (elaborated at Section 3). To find reference solutions, a representative period is established, which inherits the initial and final levels of each lake in 2011, as well as their inflows during the period, respectively sketched in Figure 4 and Figure 5.

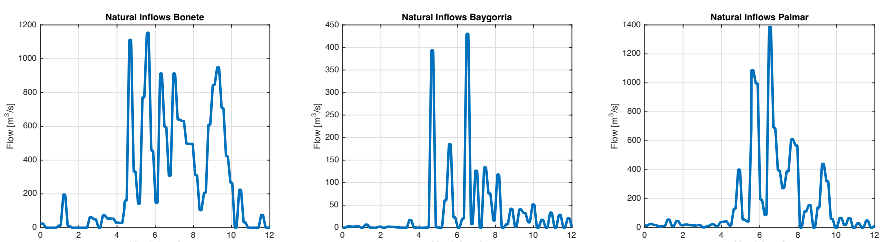

Fig. 5. Natural Inflows to the lake of every hydroelectric unit over the Río Negro [2011].

Afterwards, a reference demand profile was needed. The available ten years of hydraulic data only overlaps the early stages of Uruguay's renewable energy expansion. To create a representative demand scenario (scenario A), the 2018 residual demand was used, as wind power was fully deployed by then, and its average inflows closely matched the ten-year dataset. Additionally, another synthetic demand was crafted (demand scenario B), in this case after copying the shape of the recorded production at the Río Negro during 2011. The second instance was scaled to match the accumulated energy of the demand in the previous scenario. To determine optimized solutions for both scenarios, an iterative optimization algorithm employing successive approximations was used. We remark here how the spilling was managed for demand instances A and B. The Figure 6 sketches the result for the three solutions (red, blue and yellow curves) of better quality (i.e., energy production) resulting from the iterative algorithm previously mentioned. The results are for instance B, since it is slightly more extreme in terms of spilling. Note that the maximum flow spilled at Bonete is under 400 [m^3/s] at any time for the three solutions, a figure remarkably low, below the 10% of its technical limit. The relative gap is similar regarding Baygorria.

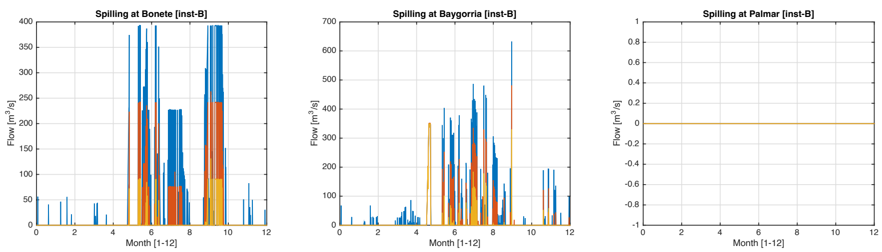

Fig. 6. Spilling graphic for the three better solutions found for demand instance B.

Regarding Palmar, no spillages are recorded in any solution across both instances. This behavior is the cornerstone to simplify the model.

3 MIP APPROACH FOR RÍO NEGRO's COMPLEX

The section introduces a MIP model to optimize the Unit Commitment and Dispatch at the Río Negro Hydroelectric Complex. In Section 2.1, optimized electricity production solutions were identified under the hydrological conditions of a dry year (in terms of natural influxes). From these, six high-quality solutions were selected, all using the same inflow series. Three of these solutions were based on an annual demand scenario derived from the actual residual demand of 2018 (scenario A), while the other three adapted the production pattern from the 2011 energy series (scenario B). A year is composed of 24 consecutive fifteen-day periods, plus a remainder with a few days more. To obtain references of efficiently managed production at Río Negro during drought conditions, the six one-year-long solutions were chopped into fifteen-day periods. This produced a reference set of 144 fifteen-day control periods. Addends P_t in Eq. (3) are polynomials, each consisting of 18 monomials. However, since $y_{3h,t}$ is zero for every t across all 144 solutions (as spilling at Palmar is nil), the monomials $p_3^{(4)} x_{3h,t} y_{3h,t}$, $p_3^{(5)} x_{3h,t} y_{3h,t}{}^2$ and $2p_3^{(5)} x_{3h,t}{}^2 y_{3h,t}$ can be disregarded. Additionally, across all 144 solutions, we checked that the combined relative influence of terms: $-p_1^{(4)} x_{1h,t} y_{1h,t}$, $-p_2^{(2)} x_{2h,t} y_{2h,t}$ and $p_3^{(5)} x_{3h,t}^3$ was negligible.

Therefore, equation (3), which provides a high-quality approximation of Río Negro's production under any weather conditions, can be simplified to the twelve monomials in equation (5) when the problem is considered within a sliding window during a mid-term dry weather season.

$$\hat{P}(x_{1h}, v_{1h}, x_{2h}, x_{3h}, v_{3h}) = \sum_{t=1}^{T} \hat{p}_1^{(1)} x_{1h,t} + \hat{p}_1^{(2)} x_{1h,t} v_{1h,t} - \hat{p}_1^{(3)} x_{1h,t} v_{1h,t}^2 - \hat{p}_1^{(4)} x_{1h,t}^2 + \hat{p}_2^{(1)} x_{2h,t} \\ - \hat{p}_2^{(2)} x_{2h,t}^2 - \hat{p}_2^{(3)} x_{2h,t} v_{3h,t} + \hat{p}_2^{(4)} x_{2h,t} v_{3h,t}^2 + \hat{p}_3^{(1)} x_{3h,t} + \hat{p}_3^{(2)} x_{3h,t} v_{3h,t} - \hat{p}_3^{(3)} x_{3h,t} v_{3h,t}^2 - \hat{p}_3^{(4)} x_{3h,t}^2 \quad . \tag{5}$$

Note that constants $p_i^{(j)}$ in Eq. (3) are renamed to $\hat{p}_i^{(j)}$ in Eq. (5). Their values were slightly adjusted to obtain a better match between the new/simplified model and the former over the six solutions found. For simplicity, the optimization problem discussed in this article includes only the opportunity cost of water at Bonete and Palmar reservoirs (i.e., Bellman costs coming from longer term planning models), as well as the penalty (i.e., cost of failure) for each MWh of unmet dispatch at every hour. This is expressed as shown in Eq. (6).

$$\begin{cases} \min\limits_{x_{ih}, y_{ih}, v_{ih}} ca_{1h}(v_{1h,0} - v_{1h,T}) + ca_{3h}(v_{3h,0} - v_{3h,T}) + CF \sum_{t=1}^{T} (d_t - g_{h,t}) & \\ d_t \geq g_{h,t}, & (i) \\ g_{h,t} = g_{1h,t} + g_{2h,t} + g_{3h,t}, & (ii) \\ g_{1h,t} = Pt\hat{B}on(x_{1h,t}, y_{1h,t}, v_{1h,t}), & (iii) \\ g_{2h,t} = Pt\hat{B}ay(x_{2h,t}, y_{2h,t}, v_{3h,t}), & (iv) \\ g_{3h,t} = Pt\hat{P}al(x_{3h,t}, y_{3h,t}, v_{3h,t}), & (v) \\ v_{1h,t} = v_{1h,t-1} + 3600(a_{1h,t} - x_{1h,t} - y_{1h,t}), & (vi) \\ x_{2h,t} + y_{2h,t} = a_{2h,t} + x_{1h,t-8} + y_{1h,t-8}, & (vii) \\ v_{3h,t} = v_{3h,t-1} + 3600(a_{3h,t} - x_{3h,t} - y_{3h,t} + x_{2h,t-16} + y_{2h,t-16}), & (viii) \\ (x_{ih}, y_{ih}, v_{ih}) \in (X, Y, V), & (ix) \end{cases} \tag{6}$$

As it was elaborated in Section 1.2, this model assumes the existence of Bellman costs to estimate the cost of opportunity of the water. In the objective function of (6), ca_{1h} and ca_{3h} (expressed in [USD/m^3]) respectively quantify those costs for Bonete and Palmar. The end-to-end variation of volume at reservoirs (i.e., $(v_{1h,0} - v_{1h,T})$ and $(v_{3h,0} - v_{3h,T})$) times its opportunity-cost are two of the costs accounted; the third is the total cost of failure.

In terms of constraints, Eq. (6)$-(i)$ ensures that the generation $g_{h,t}$ does not exceed the demand d_t at any time, which is essentially the same as Eq. (4)$-(i)$. Equations (6)$-(ii)$ to (v) represent that the total hydroelectric energy $g_{h,t}$ at any time-slot t, is the sum of the production from Bonete ($g_{1h,t}$), Baygorria ($g_{2h,t}$) and Palmar ($g_{3h,t}$).

Equations (6)$-(vi)$ to $(viii)$ enforce mass balance at each reservoir. Rain in remote areas takes days to reach the reservoir and impact storage. With permanent collection of rainfall data across the basin, natural inflows can be treated as deterministic for dispatch planning purposes. Therefore, is assumed that the inflows to the reservoirs are given: $a_{1h,t}$ (for Bonente), $a_{2h,t}$ (for Baygorria) and $a_{3h,t}$ (for Palmar). Equation (6)$-(vi)$ states that the water volume in Bonete's reservoir at time $t + 1$ must equal the volume at time t, plus the natural inflows during that period, minus the discharges. The net inflow per second $(a_{1h,t} - x_{1h,t} - y_{1h,t})$ –expressed in [m^3/s]– must be multiplied by the number of seconds in the time-slot, which in this case is 3600 (one hour). Since Baygorria is a run-of-the-river hydroelectric station, inflows and outflows must always match. Additionally, the balance at Baygorria must account for the water discharged from Bonete eight hours earlier, as indicated in the last column of Table 1 and captured in Eq. (6)$-(vii)$. The balance at Palmar's reservoir is similar (Eq. (6)$-(viii)$). Finally, Eq. (6)$-(ix)$ incorporates the technical limits of the units within the complex. The formulation in Eq. (6) is nonlinear, because even being simpler, the production addends at (5) are not linear yet. The terms in Eq. (5) can be regrouped to identify each unit, as in Eq. (7).

$$\begin{cases} Pt\hat{B}on = (\hat{p}_1^{(1)} x_{1h} - \hat{p}_1^{(4)} x_{1h}^2) + (\hat{p}_1^{(2)} v_{1h} - \hat{p}_1^{(3)} v_{1h}^2) x_{1h} \\ Pt\hat{B}ay = (\hat{p}_2^{(1)} x_{2h} - \hat{p}_2^{(2)} x_{2h}^2) - (\hat{p}_2^{(3)} v_{3h} - \hat{p}_2^{(4)} v_{3h}^2) x_{2h} \\ Pt\hat{P}al\ = (\hat{p}_3^{(1)} x_{3h} - \hat{p}_3^{(4)} x_{3h}^2) + (\hat{p}_3^{(2)} v_{3h} - \hat{p}_3^{(3)} v_{3h}^2) x_{3h} \end{cases} \tag{7}$$

These expressions complete the formulation in Eq. (6). Observe that the first term in the three production functions are analogous, and correspond to degree two polynomials $(\hat{p}x_{ih,t} - \hat{q}x_{ih,t}^2)$ in x_{ih}, all of which are concave. A concave function within a maximization process can easily and efficiently be captured by means of tangents. That idea is used to capture $(\hat{p}_3^{(1)} x_{3h} - \hat{p}_3^{(4)} x_{3h}^2)$ for Palmar with three tangents: one at the minimum technical (0); one at at the maximum technical; the other exactly in the middle. Hence, finding a good approach for that term is equivalent to maximizing a variable z_{3h}, while keeping it below these three tangents at any time:

$$\begin{cases} z_{3h,t} \le \hat{r}_3^{(1)} x_{3h,t}, \\ z_{3h,t} \le \hat{r}_3^{(2)} x_{3h,t} + \hat{s}_3^{(2)}, \\ z_{3h,t} \le \hat{r}_3^{(3)} x_{3h,t} + \hat{s}_3^{(3)} \end{cases} \tag{8}$$

The solution was similar for Bonete (z_{1h}) and Baygorria (z_{2h}), but even simpler, as only two tangent lines were needed to achieve the desired accuracy. Up to this point, only continuous variables were used. Boolean variables are now introduced to account for the expressions $(\hat{p}_1^{(2)} v_{1h} - \hat{p}_1^{(3)} v_{1h}^2) x_{1h}$ and $(\hat{p}_3^{(2)} v_{3h} - \hat{p}_3^{(3)} v_{3h}^2) x_{3h}$ of (7). These terms respectively swell the efficiency of Bonete and Palmar, by incorporating the additional energy given from the extra height as the reservoir volume expands. Next, the focus is set upon how the issue was addressed at Bonete, with a similar approach applied to Palmar.

The approach quantizes Bonete's reservoir levels and introduces variables to capture additional efficiency. These variables activate or deactivate sequentially as the reservoir volume crosses certain thresholds, which are relative to the initial volume $v_{1h,0}$. Due to Bonete's large size, volume changes over a fifteen-day period are expected to be minimal.

After analyzing the volume series of Bonete ($v_{1h,t}$) across our reference set of 144 solutions, the conclusion is that three levels were sufficient to achieve the desired accuracy. Let's denote the three levels into which Bonete's volume is quantized –after the initial volume $v_{1h,0}$ for a given fifteen-day short-term instance– as: $\overline{V1h1}$, $\overline{V1h2}$ and $\overline{V1h3}$. The approximation to $g_{1h,t}$ follows the replacement of Eq. (4)$-(iii)$ with the following set of constraints

$$\begin{cases} g_{1h,t} = z_{1h,t} + \sum_{i=1}^{3} \theta_{1h,t}^{(i)}, & (i) \\ z_{1h,t} \leq \hat{r}_1^{(1)} x_{1h,t}, & (ii) \\ z_{1h,t} \leq \hat{r}_1^{(2)} x_{1h,t} + \hat{s}_1^{(2)} & (iii) \end{cases} . \tag{9}$$

The $z_{1h,t}$ addend approximates the concave portion, as shown for Palmar in Eq. (8), thought this case only uses two tangents. The variables $\theta_{1h,t}^{(i)}$ correspond to the additional production due to the extra height. To work properly, these variables require constraints as in Eq. (10).

$$\begin{cases} 0 \leq \theta_{1h,t}^{(1)} \leq (\hat{p}_1^{(2)} \overline{V1h1} - \hat{p}_1^{(3)} \overline{V1h1}^2) x_{1h,t}, & (i) \\ 0 \leq \theta_{1h,t}^{(2)} \leq (\hat{p}_1^{(2)} \Delta\overline{V1h2} - \hat{p}_1^{(3)} \Delta\overline{V1h2}^2) x_{1h,t}, & (ii) \\ 0 \leq \theta_{1h,t}^{(2)} \leq 680(\hat{p}_1^{(2)} \Delta\overline{V1h2} - \hat{p}_1^{(3)} \Delta\overline{V1h2}^2) \varphi_{1h,t}^{(1)}, & (iii) \\ 0 \leq \theta_{1h,t}^{(3)} \leq (\hat{p}_1^{(2)} \Delta\overline{V1h3} - \hat{p}_1^{(3)} \Delta\overline{V1h3}^2) x_{1h,t}, & (iv) \\ 0 \leq \theta_{1h,t}^{(3)} \leq 680(\hat{p}_1^{(2)} \Delta\overline{V1h3} - \hat{p}_1^{(3)} \Delta\overline{V1h3}^2) \varphi_{1h,t}^{(2)} & (v) \end{cases} \tag{10}$$

This equation introduces constants derived from $\overline{V1h1}$ to $\overline{V1h3}$, which are: $\Delta\overline{V1h2} = (\overline{V1h2} - \overline{V1h1})$, $\Delta\overline{V1h2}^2 = (\overline{V1h2}^2 - \overline{V1h1}^2)$, $\Delta\overline{V1h3} = (\overline{V1h3} - \overline{V1h2})$ and $\Delta\overline{V1h3}^2 = (\overline{V1h3}^2 - \overline{V1h2}^2)$. Equation (10)$-(i)$, which is linear, allows $\theta_{1h,t}^{(1)}$ to take on a value similar to $(\hat{p}_1^{(2)} v_{1h} - \hat{p}_1^{(3)} v_{1h}^2) x_{1h}$ in Eq. (7). These values align precisely when $v_{1h,t} = \overline{V1h1}$. For now, keep in mind that $\varphi_{1h,t}^{(1)} = 1$ only if $v_{1h,t} \geq \overline{V1h2}$, and $\varphi_{1h,t}^{(2)} = 1$ only if $v_{1h,t} \geq \overline{V1h3}$. If $\varphi_{1h,t}^{(1)} = 0$, Eq. (10)$-(iii)$ forces $\theta_{1h,t}^{(2)} = 0$. The deactivation of $\varphi_{1h,t}^{(2)}$ similarly affects $\theta_{1h,t}^{(3)}$ due to Eq. (10)$-(v)$. Conversely, since 680 [m^3/s] is the maximum technical turbinated flow for Bonete, Eq. (10)$-(iii)$ deactivates when $\varphi_{1h,t}^{(1)} = 1$, and as $x_{1h,t}$ changes, the sum of $\theta_{1h,t}^{(1)} + \theta_{1h,t}^{(2)}$ approximates $(\hat{p}_1^{(2)} v_{1h} - \hat{p}_1^{(3)} v_{1h}^2) x_{1h}$ when the reservoir volume is around $\overline{V1h2}$. A similar trigger effect occurs when $\varphi_{1h,t}^{(2)} = 1$, which also implies that $\varphi_{1h,t}^{(1)} = 1$. In this case, $\sum_{i=1}^{3} \theta_{1h,t}^{(i)}$ approximates $(\hat{p}_1^{(2)} v_{1h} - \hat{p}_1^{(3)} v_{1h}^2) x_{1h}$ when the reservoir volume is near $\overline{V1h3}$. Equation (11) shows how $\varphi_{1h,t}^{(i)}$ variables can be forced to zero according on thresholds.

$$\begin{cases} \varphi_{1h,t}^{(1)} \leq 1 - \dfrac{\overline{V1h2} - v_{1h,t}}{M1}, \\ \varphi_{1h,t}^{(2)} \leq 1 - \dfrac{\overline{V1h3} - v_{1h,t}}{M1} \end{cases} \tag{11}$$

Note that, with a properly chosen value of $M1$, $\varphi_{1h,t}^{(1)}$ cannot be activated if $v_{1h,t} < \overline{V1h2}$, as it is a boolean variable constrained to a value less than 1. The same idea goes for $\varphi^{(2)}_{1h,t}$. The strategy for addressing the problem at Palmar is similar. The main difference lies in Palmar's faster dynamics and smaller reservoir, which allows its lake level to fluctuate more significantly than Bonete's. To account for this, five reservoir levels were used for Palmar instead of three.

The only remaining unresolved term is $-(\hat{p}^{(3)}_2 v_{3h} - \hat{p}^{(4)}_2 v^2_{3h})x_{2h}$, which impacts Baygorria's efficiency as the level of Palmar's lake rises. Experimental evaluations –both on the 144 prior solutions and on the results of test models prior to this one– have shown that Palmar's power and reservoir size dominate the optimization outcome. It is Palmar's reservoir management that influences Baygorria, not the other way around. Therefore, the subproblem was handled through a simple linear regression of the expression. The regression is performed for each specific instance before running the problem, using the five designated level thresholds $\overline{V3h1}$ to $\overline{V3h5}$ for Palmar in that instance.

4 EXPERIMENTAL EVALUATION

The evaluation of the MIP model was conducted using a test-set of 204 instances. These instances were grouped into 6 subgroups, each consisting of 34 instances. The subgroups are fifteen-day periods sampled over the three reference good-quality solutions of scenario A as defined in Section 2.2, meaning that the profile of residual demands match actual data from 2018. The first half of the instances replicates the residual demand, while the second half increases it by a factor of 1.5 and adds a sustained demand of an additional 50 MW, as in Table 2.

Subgroup	ca_{1h} [USD/m^3]	ca_{3h} [USD/m^3]	CF [USD/MWh]	Residual Demand
1	0.0033	0.0063	3200	d_t as in 2018
2	0.0063	0.0033	3200	d_t as in 2018
3	0.0048	0.0048	3200	d_t as in 2018
4	0.0033	0.0063	1600	50 MW + 1.5 × d_t
5	0.0063	0.0033	1600	50 MW + 1.5 × d_t
6	0.0048	0.0048	1600	50 MW + 1.5 × d_t

Table 2. Complementary parameters to complete the test-instances data-set.

Note that sampling among different solutions allow exploring changes in the initial conditions of reservoirs of Bonete and Palmar, while natural inflows do the proper with the series of natural inflows sketched in Figure 5. The economical parameters ca_{1h}, ca_{3h} and CF derive from the actual hydro-production during 2011 for a reference cost of energy of 80 [USD/MWh]. Bellman values ca_{1h} and ca_{3h} are equal at instances 3 and 6, whereas other instances shift toward either Bonete or Palmar. The cost of failure for the last three subgroups is 20 times the reference energy cost, and it is doubled for the first half.

Instances were solved by means of the software `IBM(R) ILOG(R) CPLEX(R) Interactive Optimizer 12.6.3.0`, running on an `HP ProLiant DL385 G7`, with `AMD Opteron` processor 6172, 24 cores at 2.1GHz and 64GB of RAM.

All solutions reported here reached optimality, with relative differences between the cumulated reference production function in (3) and its equivalent $\sum_{t=1}^{T} g_{h,t}$ of the MIP's approximation (eq-(6)$-(ii)$) ranging from -0.012% to 0.046%, with average -0.001%, which is negligible. When we move from total energy to power (i.e., slot-by-slot energy) the difference in [MWh] ranges from 0.92 to 32.05, with a mean of 12.52. As a reference, consider that the combined installed plant of Bonete, Baygorria and Palmar is 603 MW. The maximum deviation in power occurs for the 10th instance of subgroup 4 in Table 2, and its corresponding curves are shown in Figure 7.

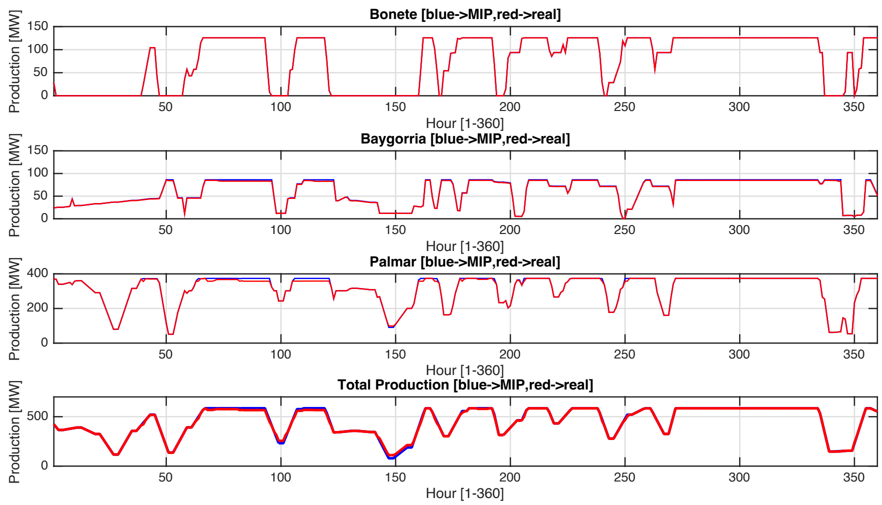

Fig. 7. Real [(3) in red] vs MIP approximated production: $g_{1h,t}$, $g_{2h,t}$, $g_{3h,t}$ and $g_{h,t}$.

Computation times ranged from under 1 to 1210 seconds, with an average of 121 seconds. Notably, in most cases, the majority of the time was spent on fine-tuning the solution to reach optimality. We remark that in over 95% of the 204 instances solved, a feasible solution with a proven duality gap (i.e., an error estimate) of less than 1% was achieved within the first 2 seconds of runtime.

5 CONCLUSIONS AND FUTURE WORK

Merging conventional renewable energy sources with newer ones allows for the best use of both, but poses challenges in operations. MIP and MISP models are ideal for addressing parts of the problem and are better suited to adapt to emerging challenges. This is not the case for legacy hydroelectric complexes such as the one in Río Negro. This paper presents a MIP model for such a complex that effectively tackles the subproblem. This research team is actively working to incorporate additional components into the model to develop a more comprehensive and realistic Unit Commitment and Dispatch Optimization system.

Acknowledgments. This work was supported by UTE (Administración Nacional de Usinas y Trasmisiones Eléctricas, Uruguay) and PEDECIBA (Programa de Desarrollo de las Ciencias Básicas, Uruguay).

References

1. Bertoni, R., Messina, P.: The "wind revolution" in Uruguay and the role of the public sector in guiding energy transitions. In: Energy Transitions in Latin America: The Tough Route to Sustainable Development, pp. 195–216. Springer (2023)
2. Bouzas, B., Teliz, E., Díaz, V.: Green hydrogen production in Uruguay: a techno-economic approach. International Journal of Chemical Reactor Engineering **22**(7), 783–795 (2024)
3. Casaravilla, G., Chaer, R.: Energy transition of Uruguay. In: IAEE Energy Forum, Fourth Quarter 2021, pp, 11-14. International Association for Energy Economics (2021)
4. Cristobal, M.P., Escudero, L.F., Monge, J.F.: On stochastic dynamic programming for solving large-scale planning problems under uncertainty. Computers & Operations Research **36**(8), 2418–2428 (2009)
5. Diniz, A.L., Souza, T.M.: Short-term hydrothermal dispatch with river-level and routing constraints. IEEE Transactions on Power Systems **29**(5), 2427–2435 (2014)
6. Ferrero, R., Rivera, J., Shahidehpour, S.: A dynamic programming two-stage algorithm for long-term hydrothermal scheduling of multireservoir systems. IEEE Transactions on Power Systems **13**(4), 1534–1540 (1998)
7. Hargreaves, J.J., Hobbs, B.F.: Commitment and dispatch with uncertain wind generation by dynamic programming. IEEE Transactions on sustainable energy **3**(4), 724–734 (2012)
8. Khatami, R., Parvania, M., Chen, C., Guggilam, S.S., Dhople, S.V.: Dynamics-aware continuous-time economic dispatch: A solution for optimal frequency regulation. In: HICSS. pp. 1–10 (2020)
9. MOP: Modelo de operación desarrollado por UTE (2024), https://gitlab.com/utepladmm/MOP, accessed: 2024-09-21
10. Oroño, D., Vignolo, M., Echinope, V.: Analysis of the penetration and impacts of hybrid and electric vehicles in the electrical system of Uruguay. In: 2015 IEEE PES Innovative Smart Grid Technologies Latin America (ISGT LATAM). pp. 75–80. IEEE (2015)
11. Patrone, J., Plat, A., Failache, G.: Actualización de los criterios de operación durante crecidas normales y extraordinarias de los embalses en cadena del Río Negro (Uruguay). In: Dam Maintenance and Rehabilitation, pp. 433–440. Routledge (2017)
12. REN21: Renewables 2020 global status report. Tech. rep., Paris: REN21 Secretariat (2021), https://www.ren21.net/gsr-2020/
13. Risso, C.: Benefits of demands control in a smart-grid to compensate the volatility of non-conventional energies. Revista Facultad de Ingeniería Universidad de Antioquia (93), 19–31 (aug 2019). https://doi.org/10.17533/udea.redin.20190404, https://revistas.udea.edu.co/index.php/ingenieria/article/view/336255
14. Sherkat, V., Campo, R., Moslehi, K., Lo, E.: Stochastic long-term hydrothermal optimization for a multireservoir system. IEEE Transactions on Power Apparatus and Systems (8), 2040–2050 (1985)
15. U.S. Energy Information Administration: Uruguay - international - u.s. energy information administration (eia) (2024), https://www.eia.gov/international/data/country/URY/electricity/electricity-generation, accessed: 2024-09-17
16. Van Ackooij, W., Danti Lopez, I., Frangioni, A., Lacalandra, F., Tahanan, M.: Large-scale unit commitment under uncertainty: an updated literature survey. Annals of Operations Research **271**(1), 11–85 (2018)